24th ABCM International Congress of Mechanical Engineering
December 3-8, 2017, Curitiba, PR, Brazil

COBEM-2017-2179
NUMERICAL AND EXPERIMENTAL ANALYSIS OF A COPPER THERMOSYPHON

Larissa Krambeck
Thiago Antonini Alves
Laboratory of Thermal Control (LabTC), Federal University of Technology – Paraná (UTFPR), Av. Monteiro Lobato, s/n°, km 04, CEP 84.016-210, Ponta Grossa/PR, Brazil
thiagoaalves@utfpr.edu.br

Caroline Rezende Machado
Fernanda Anschau Domingues Cabral
Alex Vinicius Lopes Machado
Paulo Henrique Dias dos Santos
Multiphase Flow Research Center (NUEM), Federal University of Technology – Paraná (UTFPR), Rua Deputado Heitor Alencar Furtado 5000, Bloco N, CEP 81.280-340, Curitiba, Brazil
psantos@utfpr.edu.br

Abstract. *In this paper, a numerical and experimental analysis of the thermal behavior of copper thermosyphon was performed. The thermosyphon was produced by copper tube ASTM B75 Alloy 122 with an outer diameter of 9.45 mm, an inner diameter of 7.75 mm, and a length of 200 mm. The analysis was made with a filling ratio of 100% of the evaporator volume. The working fluid was deionized water. The experimental tests were done for the thermosyphon in the vertical position under thermal loads between 5 and 45 W. It was implemented a numerical modeling in order to simulate the details of the two-phase flow and heat transfer phenomena during the operation of the thermosyphon. The volume of the fluid (VOF) model in ANSYS/FLUENT was used for the simulation. The evaporation, condensation, and phase change processes in the thermosyphon were implemented into the code of FLUENT by User-Defined Function (UDF). The simulation results were compared with experimental measurements at the same condition. The simulation was successful in reproducing the heat and mass transfer processes in a thermosyphon.*

Keywords: *Thermosyphon, Experimental, Numerical Modeling, ANSYS/FLUENT.*

1. INTRODUCTION

Thermosyphons are highly efficient passive heat transfer devices capable of transferring large amounts of heat with a small temperature difference. The reason for this phenomenon is the use of latent heat of vaporization. These devices are constituted of an evacuated metal tube filled with a working fluid. They use the gravity for the internal fluid circulation. Thermosyphons are used to improve the heat transfer in many industrial fields such as electronics, telecommunications, aerospace, food, among others (Faghri, 2014).

The thermosyphons have three regions with distinct roles in their operation, they are evaporator, adiabatic section, and condenser. The evaporator, the lower region of the tube, is heated by a hot source and the working fluid undergoes an evaporation process. This steam, because of the pressure difference, moves to the colder region (condenser). In this region, the steam generated in the evaporator loses energy as heat and is condensed. The working fluid, in the liquid state, flows back to the evaporator by gravity, closing the cycle. The adiabatic section is located between the evaporator and the condenser. In this section, there isn't heat transfer between the thermosyphon and the environment. In some cases, the adiabatic section is absent (Groll and Rösler, 1992). A schematic diagram of the thermosyphon operating principle is shown in Fig. 1 (Santos *et al.*, 2017). More details of the thermosyphons can be found in Chi (1976), Peterson (1994), Mantelli (2013), and Reay *et al*. (2014).

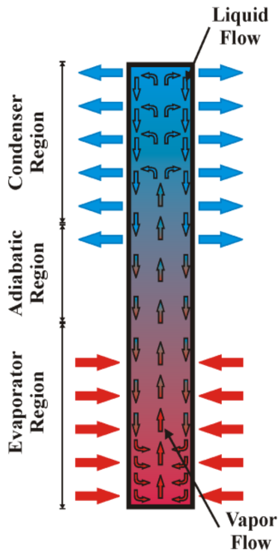

Figure 1. Schematic diagram of the thermosyphon operating principle

Some researchers have been studying the evaporation phenomena, which occur in evaporators of thermosyphons (Alizadehdakhel *et al.*, 2010; Fadhl *et al.*, 2013; and Fadhl *et al.*, 2015). However, they do not present a study of the numerical heat transfer coefficient during the boiling phenomena. Thus, this paper aims to present a numerical and experimental study of the boiling heat transfer coefficient related to the evaporator of thermosyphons in order to obtain a numerical correlation.

2. EXPERIMENTAL AND NUMERICAL PROCEDURE

2.1 Experiment

The thermosyphon was produced by copper tube ASTM B75 Alloy 122 with an outer diameter of 9.45 mm, an inner diameter of 7.75 mm and, a length of 200 mm. The thermosyphon has an evaporator of 80 mm in length, an adiabatic region of 20 mm in length and, a condenser of 100 mm in length. The working fluid used was deionized water with a filling ratio of 100% of the evaporator volume. Table 1 presents the main features of the thermosyphon and the working fluid.

Table 1 – Main characteristics of the thermosyphon.

Characteristics	**Dimension**
Thermosyphon inner diameter [mm]	7.75
Thermosyphon outer diameter [mm]	9.45
Evaporator length [mm]	80.0
Adiabatic section length [mm]	20.0
Condenser length [mm]	100
Working fluid	Deionized water
Filling ratio [%]	100
Volume of working fluid [ml]	3.77

The experimental apparatus used for the experimental tests are shown in Fig. 2. It is composed of a power supply unit (*Agilent*™ U8002A), a data logger (*Agilent*™ 34970A with 20 channels), a *Dell*™ desktop, a fan (*Ultrar*™), an uninterruptible power supply (*NHS*™), and a universal support. For the evaluation of the thermal performance of the thermosyphon, K-type thermocouples *Omega™* were used. More details of the experimental procedure can be found in Aguiar (2016).

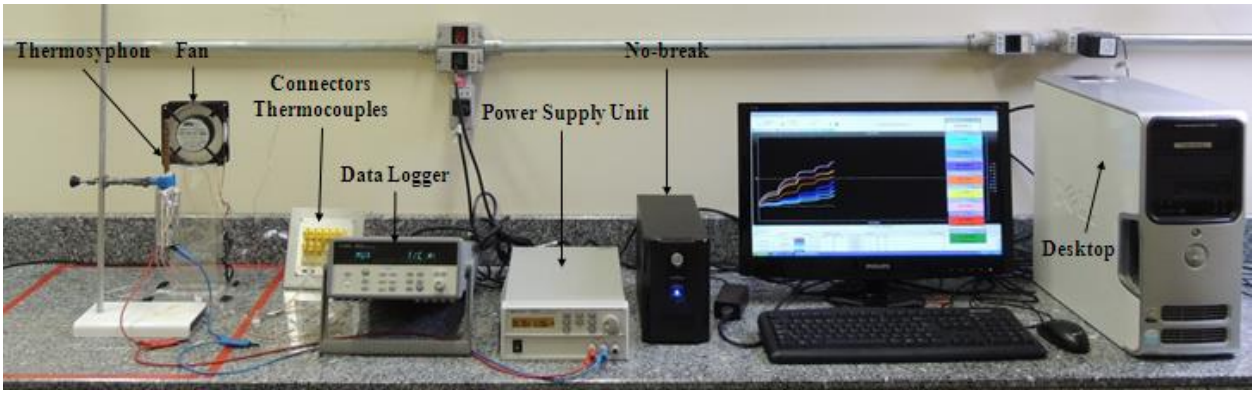

Figure 2. Experimental Apparatus

2.2 Numerical Model

The governing equations of mass continuity, momentum, and energy were used to describe the motion of the working fluid in a thermosyphon. The continuity equation of the Volume of the Fluid (VOF) Model for the second phase (L) can be expressed as:

$$\nabla.\left(\alpha_L \rho_L \vec{u}\right) + \frac{\partial\left(\alpha_L \rho_L\right)}{\partial} = S_m \,, \tag{1}$$

where, S_m is the mass source term used to calculate the mass transfer during evaporation and condensation.

The momentum equation for the VOF Model takes the following form:

$$\frac{\partial\left(\rho\vec{u}\right)}{\partial t} + \nabla.\left(\rho\vec{u}\vec{u}\right) = \rho\vec{g} - \nabla p + \nabla.\left[\mu\left(\nabla\vec{u} + \nabla\vec{u}^{T}\right) - \frac{2}{3}\mu\nabla.uI\right] + F_{CSF} \,, \tag{2}$$

where, F_{CSF} is the momentum source term which was estimated using the continuum surface force model.

The energy equation for the VOF Model has the following form:

$$\frac{\partial\left(\rho e\right)}{\partial t} + \nabla.\left(\rho e \vec{u}\right) = \nabla.\left(k.\nabla T\right) + \nabla.\left(p\vec{u}\right) + S_E \,, \tag{3}$$

where, S_E is the energy source term used to calculate the heat transfer during evaporation and condensation.

The numerical model was developed and implemented using the ANSYS/FLUENT software. The evaporation, condensation, and phase change processes in the thermosyphon were implemented by User-Defined Function (UDF) using the model published by Schepper et al. (2009) and Machado and Cabral (2017).

3. EXPERIMENTAL AND NUMERICAL PROCEDURE

3.1 Model Validation

The thermosyphon presented in the Table 1 was modeled for the numerical study discussed in Section 2.2. The element size of the bidimensional mesh was defined based on the bubble diameter of Rohsenow. The focus of the model validation was to determine the factor of mass transfer intensity of the phase-change model of Lee, implemented in the UDF. The mass transfer is determined by

$$\dot{m}_{lv} = -\dot{m}_l = r_l \alpha_l \rho_l \frac{T - T_{sat}}{T_{sat}} \,, \quad \text{if} \;\; T > T_{sat} \,, \tag{4}$$

where, r is the factor of mass transfer intensity. The factor r needs to be such to maintain the interfacial temperature close to the saturation temperature, avoiding divergence during the numerical analysis. Some researchers, Wu *et al*. (2016), De Schepper *et al*. (2009), and Alizadehdakhel *et al.* (2010), defined the factor r as 0,1 s^{-1} in their studies, but some Fang (2010) and Yang (2007) used the factor equal to 100 s^{-1}**.**

According to the validation simulations results, besides a coefficient r of 0,1 s^{-1} proved sufficient to initiate bubble nucleation in the boiling process in the evaporator, convergence errors appeared in 2 seconds, caused by an existence of a superheated region in the evaporator. The superheating is caused by the lack of condensation, that is, there is not enough fluid condensing to cool the internal surface of the thermosyphon, generating hot regions in the interface evaporator-adiabatic section. For r = 100 s^{-1}, the condensation was so intense that provoked an imbalance between the phases, due to the excess of vapor being condensed in the thermosyphon, increasing the amount of the liquid phase present.

The factor of mass transfer intensity r chosen for the further analysis was 0,1s^{-1} for the evaporation process and 1s^{-1} for the condensation. This configuration presented the perfect balance of phases and a temperature profile close to the one obtained by Aguiar (2016), observed in Fig. 3.

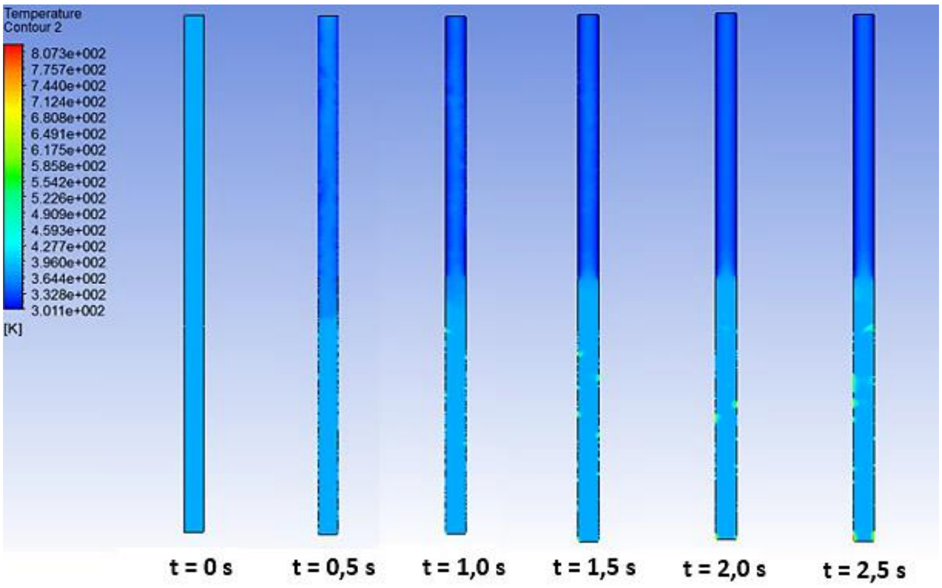

Figure 3. Temperature profile obtained during the model validation

The temperature profile is obtained for different thermal loads: 5, 10, 15, 20, 25, and 30W. Results have shown an increase of appearance of superheat regions along the evaporator with a higher thermal load, as observed in Fig. 4, while the temperatures in the condenser are constant.

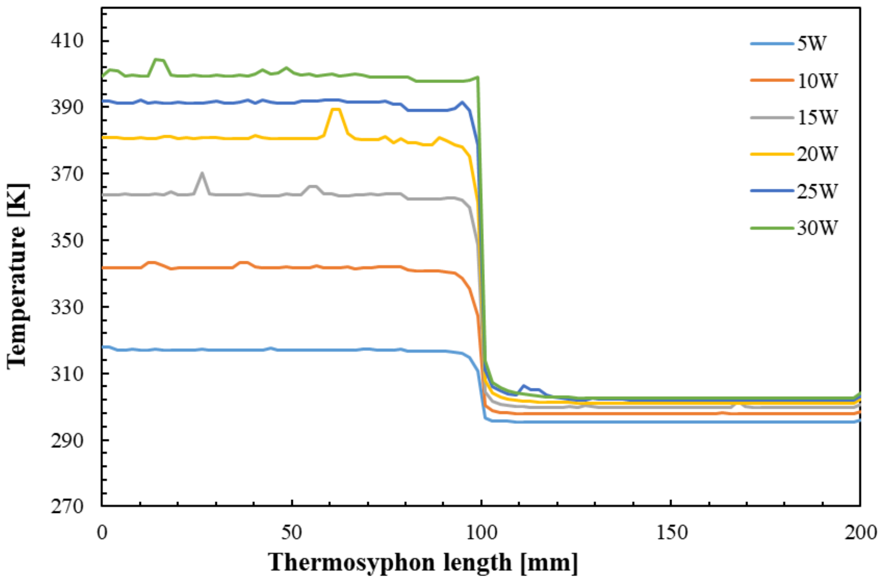

Figure 4. Distribution of temperature in a thermosyphon with 100% filling rate and different thermal loads

3.2 Filling charge ratio analysis

The study was performed for four different filling ratios: 100, 80, 60, and 40%. Figure 5 presents the comparison of the temperature distribution along the thermosyphon length for a thermal load of 20W. A minor variation between the temperatures of the evaporator was observed, where the thermosyphon with higher filling rates present a better stability and also an isothermal condition along the condenser. This behavior is justified by the fact that there was less incidence of superheated regions on those with the high filling ratio (100% and 80%), due the existence of liquid in the superior region of the evaporator to absorb latent heat.

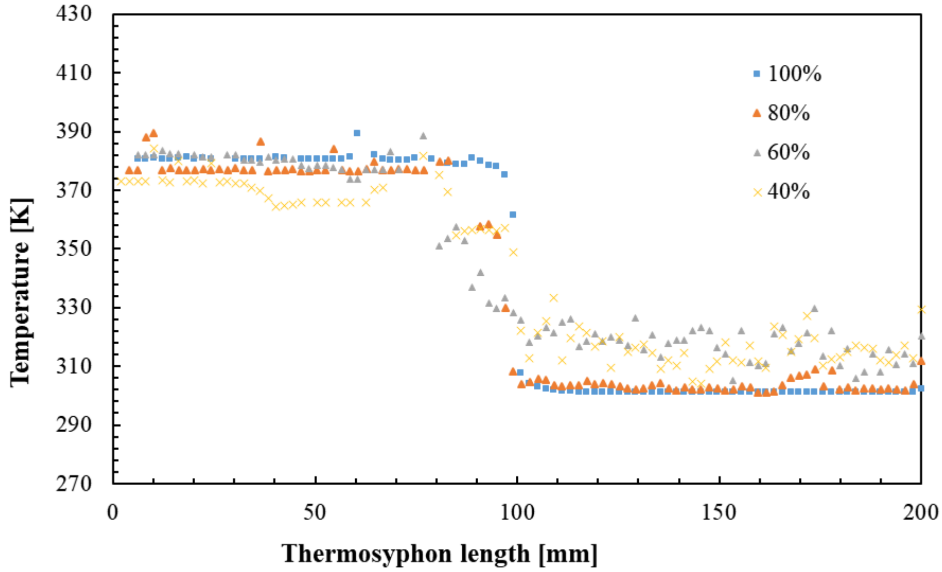

Figure 5. Comparison of filling rates for a thermal load of 20W

3.3 Boiling heat transfer coefficient

The two-phase heat transfer coefficient was determined by the local convective coefficients according to Newton's law of cooling, and the mean convective coefficient by obtaining the numerical average temperature at the surface of the evaporator. Those results were compared with the Rohsenow correlation (Rohsenow, 1951).

Figure 6 presents the results for a thermal load of 20W and filling rate of 100%, where the average convective coefficient for the Rohsenow model is 2,216.1 W/m²K and the value calculated from the average evaporator temperature is 2,934.8 W/m²K. It can be seen that the value of the Rohsenow correlation approaches the value of the calculated average convective coefficient.

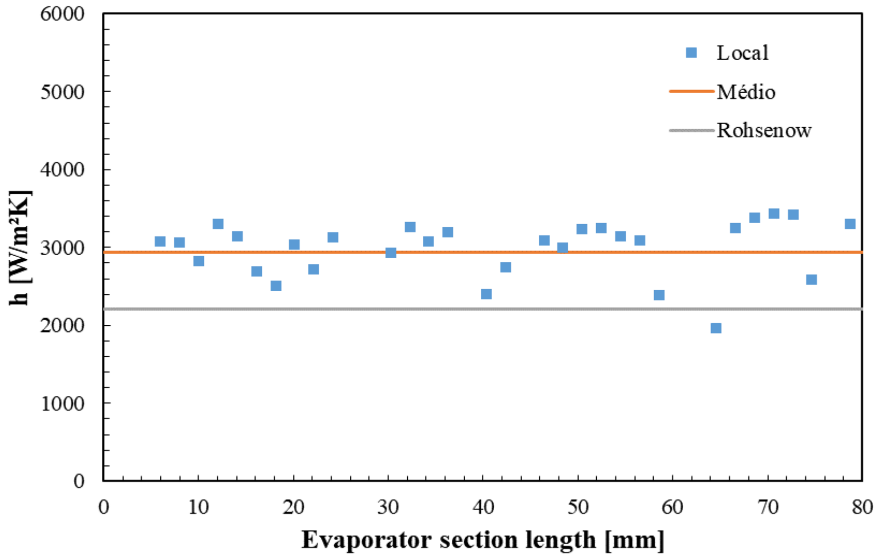

Figure 6. Convective coefficient for filling rate 100% and thermal load of 20W

The convective coefficients for lower filling rates are higher compared to 100% filling rate. Figure 7 presents the result of local and average coefficients for 80% and 20W of thermal load. The Rohsenow correlation cannot be used for filling rates different of 100%.

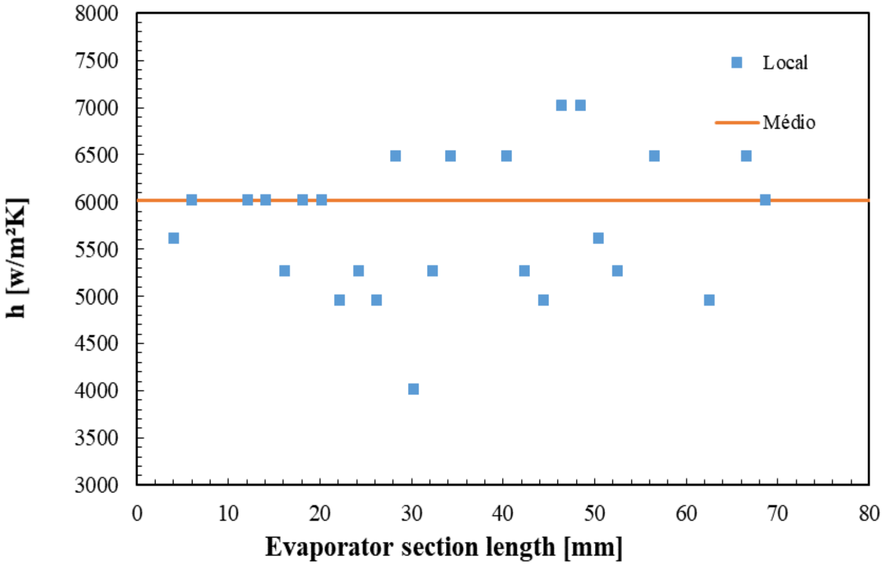

Figure 7. Convective coefficient for 80% and 20W

4. CONCLUSIONS

In this present project it was developed a methodology of numerical analysis of the pool boiling process in an evaporator section of a thermosyphon. The study of heat transfer is necessary to dimension these devices, which have great potential in industrial and residential sustainable applications, due to their high heat transfer efficiency. The methodology for numerical modeling showed satisfactory results comparing to correlations available in literature and physical tests results.

In addition, it was possible to study the effect of condensation-evaporation Lee's factor, which is widely used for numerical modeling in phase-change problems. The factor depends on the numerical model and the context of the analysis. The values commonly used in the literature have shown non-satisfactory results for the modeling of this project, once the thermosyphon has reached its operation limits.

To determine the multiphase heat transfer coefficient in the thermosyphon evaporator, the local convective coefficients for several points were calculated through Newton's law of cooling, and the average convective coefficient was calculated by obtaining the average temperature at the evaporator surface. Those values were compared with correlation of Rosehnow developed for nucleate boiling inside circular section pipes. The Rosehnow study better correlates to the simulation data for the cases that had higher heat transfer (25W and 30W). This result is expected, since in his experiment, the author evaluated only the nucleate boiling with jets and columns regime. For the analysis with low heat flux in the evaporator the regime can be classified as nucleate boiling with isolated bubbles.

The results obtained in this work show that the methodology developed is adequate for the proposed problem. The numerical data obtained in this work, as well as the proposed methodology, can feed further studies to obtain correlations to estimate the coefficient of heat transfer by convection inside the evaporator of the thermosyphon.

5. REFERENCES

Aguiar, V.M., 2016. *Influence of filling ratio and inclination angle on thermal performance of thermosyphons.* Graduation work, Federal University of Technology – Paraná, Ponta Grossa, Brazil (in Portuguese).

Alizadehdakhel, A., Rahimi, M., Alsairafi, A.A., 2010. "CFD Modeling of Flow and Heat Transfer in a Thermosyphon". *International Communications in Heat and Mass Transfer*, Vol. 37, pp. 312-318.

Chi, S.W., 1976. *Heat Pipe Theory and Practice: A Sourcebook.* Hemisphere Publishing Corporation, Washington, USA.

Fadhl, B., Wrobel, L.C., Jouhara, H., 2013. "Numerical Modelling of the Temperature Distribution in a Two-Phase Closed Thermosyphon". *Applied Thermal Engineering*, Vol. 60, pp. 122-131.

Fadhl, B., Wrobel, L.C., Jouhara, H., 2015. "CFD Modelling of a Two-Phase Closed Thermosyphon Charged with R134a and R404a". *Applied Thermal Engineering*, Vol. 78, pp. 482-490.

Faghri, A., 2014. “Heat Pipes: Review, Opportunities and Challenges”. *Frontiers in Heat Pipes*, Vol. 5, pp 01-48.

Groll, M., Rösler, S., 1992. “Operation Principles and Performance of Heat Pipes and Closed Two-Phase Thermosyphons”. *Journal of Non-Equilibrium Thermodynamics*, Vol. 17, pp. 091-151.

Machado, C.R., Cabral, F.A.D., 2017. *Methodology of numerical analysis of the pool boiling process in a closed thermosyphon evaporator*. Graduation work, Federal University of Technology – Paraná, Curitiba, Brazil (in Portuguese).

Mantelli, M.B.H., 2013. *Thermosyphon Technology for Industrial Applications*, Chapter 11, In: Vasiliev, L.L. and Kakaç, S. (Eds.), *Heat Pipes and Solid Sorption Transformations: Fundamentals and Practical Applications.* CRC Press, Boca Raton, USA.

Peterson, G. P., 1994. *An Introduction to Heat Pipes: Modeling, Testing and Applications, (Thermal Management of Microelectronic and Electronic System Series)*. Wiley-Interscience, New York, USA.

Reay, D. A., Kew, P. A., McGlen, R. J., 2014. *Heat Pipe: Theory, Design and Applications*. Butterworth-Heinemann, Amsterdam, NED.

Rohsenow, W.M., 1951. *A method of correlating heat transfer data for surface boiling of liquids*. Technical Report #5, Massachusetts Institute of Technology, Cambridge, USA.

Schepper, S. C. K., Heynderickx, G. J., Marin, G. B.. 2009. “Modeling the Evaporation of a Hydrocarbon Feedstock in the Convection Section of a Steam Cracker”. *Computers & Chemical Engineering*, Vol. 33, pp. 122-132.

Santos, P. H. D., Reis, L. S., Marquardt, L. S., Vicente, K. A. T., Antonini Alves, T., 2017. “Modeling and Experimental Tests of a Copper Thermosyphon”. *Acta Scientiarum. Technology*, Vol. 39, pp. 59-68.

Yang, Z., 2007. “Numerical and Experimental Investigation of Two Phase Flow”. *International Journal of Heat and Mass Transfer*, Vol. 51, pp. 1003-1016.

Wu, H.L., Peng, X.F., Ye, P., Eric Gong, Y., 2006. “Simulation of Refrigerant Flow Boiling in Serpentine Tubes”. *International Journal of Heat and Mass Transfer*, Vol. 50, pp. 1186–1195.

6. RESPONSIBILITY NOTICE

The authors are the only responsible for the printed material included in this paper.